A brilliant monomeric red fluorescent protein to visualize cytoskeleton dynamics in *Dictyostelium*

Markus Fischer[a], Ilka Haase[a], Evelyn Simmeth[b], Günther Gerisch[b], Annette Müller-Taubenberger[b,*]

[a] *Lehrstuhl für Organische Chemie und Biochemie, Technische Universität München, Lichtenbergstrasse 4, D-85747 Garching, Germany*
[b] *Max-Planck-Institut für Biochemie, Am Klopferspitz 18, D-82152 Martinsried, Germany*

Received 26 August 2004; accepted 22 September 2004

Available online 19 October 2004

Edited by Jesus Avila

Abstract Red fluorescent proteins (RFPs) combined with GFP are attractive probes for double-fluorescence labeling of proteins in live cells. However, the application of these proteins is restrained by stable oligomer formation and by their weak fluorescence in vivo. Previous attempts to eliminate these problems by mutagenesis of RFP from *Discosoma* (DsRed) resulted in the monomeric mRFP1 and in the tetrameric RedStar RFP, which is distinguished by its enhanced fluorescence in vivo. Based on these mutations, we have generated an enhanced monomeric RFP, mRFPmars, and report its spectral properties. Together with green fluorescent labels, we used mRFPmars to visualize filamentous actin structures and microtubules in *Dictyostelium* cells. This enhanced RFP proved to be suitable to monitor the dynamics of cytoskeletal proteins in cell motility, mitosis, and endocytosis using dual-wavelength fluorescence microscopy.

Keywords: Actin cytoskeleton; Fluorescent protein; Microtubule; Monomeric RFP; Synthetic gene; *Dictyostelium discoideum*

1. Introduction

Aequoria victoria green fluorescent protein (GFP) or variants derived from it can be fused to many proteins to study the dynamics of their translocations, interactions or conformational changes in live cells (for review see [1–5]). Among new fluorescent proteins from *Anthozoa*, those emitting in the red or far-red range are of special interest since eukaryotic cells show reduced autofluorescence at longer wavelengths. In combination with GFP, red fluorescent proteins (RFPs) are suitable for multicolor labeling and have been suggested for measuring fluorescence resonance energy transfer (FRET) [6]. However, in practice RFPs are inferior to GFP as they form oligomers and their fluorescence in vivo is low. In particular, DsRed from *Discosoma spec*. is a tetramer maturing slowly via a green intermediate and does not reach the brilliance required for high-quality imaging of eukaryotic cells [7].

The disadvantages of DsRed are increasingly being overcome by sequential mutagenesis. Firstly, monomeric mRFP1 that matures within one hour was obtained by the substitution of 50 amino acid residues in DsRed [8]. Second, tetrameric RedStar showing enhanced fluorescence in live cells has been selected from DsRed by consecutive runs of mutagenesis in bacteria and yeast, each run followed by isolation of the most strongly fluorescing cells. Seven amino acid residues turned out to be mutated in RedStar [9].

In an attempt to double-label cytoskeletal proteins in the fast growing cells of *Dictyostelium*, we did not succeed in using DsRed or mRFP1. In the case of DsRed, only green fluorescent precursors were detectable, and the fluorescence of mRFP1 was too weak to acquire images with high spatial and temporal resolution (unpublished results). Therefore, we synthesized a gene that encodes a derivative of DsRed combining the two sets of mutations that made the protein either monomeric or enhanced its fluorescence in vivo. In addition, we optimized the sequence in accord with the codon usage in the A/T-rich genome of *Dictyostelium*. The new version of DsRed named mRFPmars turned out to be a brilliant fluorescence tag for various proteins in this microorganism and may be also useful in other eukaryotes.

Here, we show that mRFPmars purified from bacteria is monomeric. The spectral properties of this protein and the emission spectrum of a fusion protein expressed in *Dictyostelium* cells are presented. To demonstrate the usefulness of mRFPmars for double-labeling and for monitoring the dynamics of protein assembly within cells, we have analyzed three fusion proteins by confocal imaging in *Dictyostelium* cells, two of them visualizing the actin-filament system and one incorporating into microtubules. Specificity of localization was tested by co-labeling the endoplasmic reticulum (ER) with calnexin-GFP. To study mitosis, the α-tubulin label was combined with histone 2B-GFP. To monitor endocytosis, an actin label was combined with a green fluorescent fluid-phase marker, Alexa 488-dextran.

2. Materials and methods

2.1. Gene synthesis

First, the overlapping oligonucleotides DDRFP-1 and DDRFP-2 (Fig. 1A) were annealed, and a double-stranded DNA segment of 111 bps was obtained by extension using EXT DNA polymerase (Finnzyme, Epsoo, Finland). Subsequently, in a sequence of seven PCR amplifications the complete mRFPmars gene was synthesized. The

* Corresponding author. Fax: +49-89-8578-3885.
E-mail address: amueller@biochem.mpg.de (A. Müller-Taubenberger).

0014-5793/$22.00
doi:10.1016/j.febslet.2004.09.084

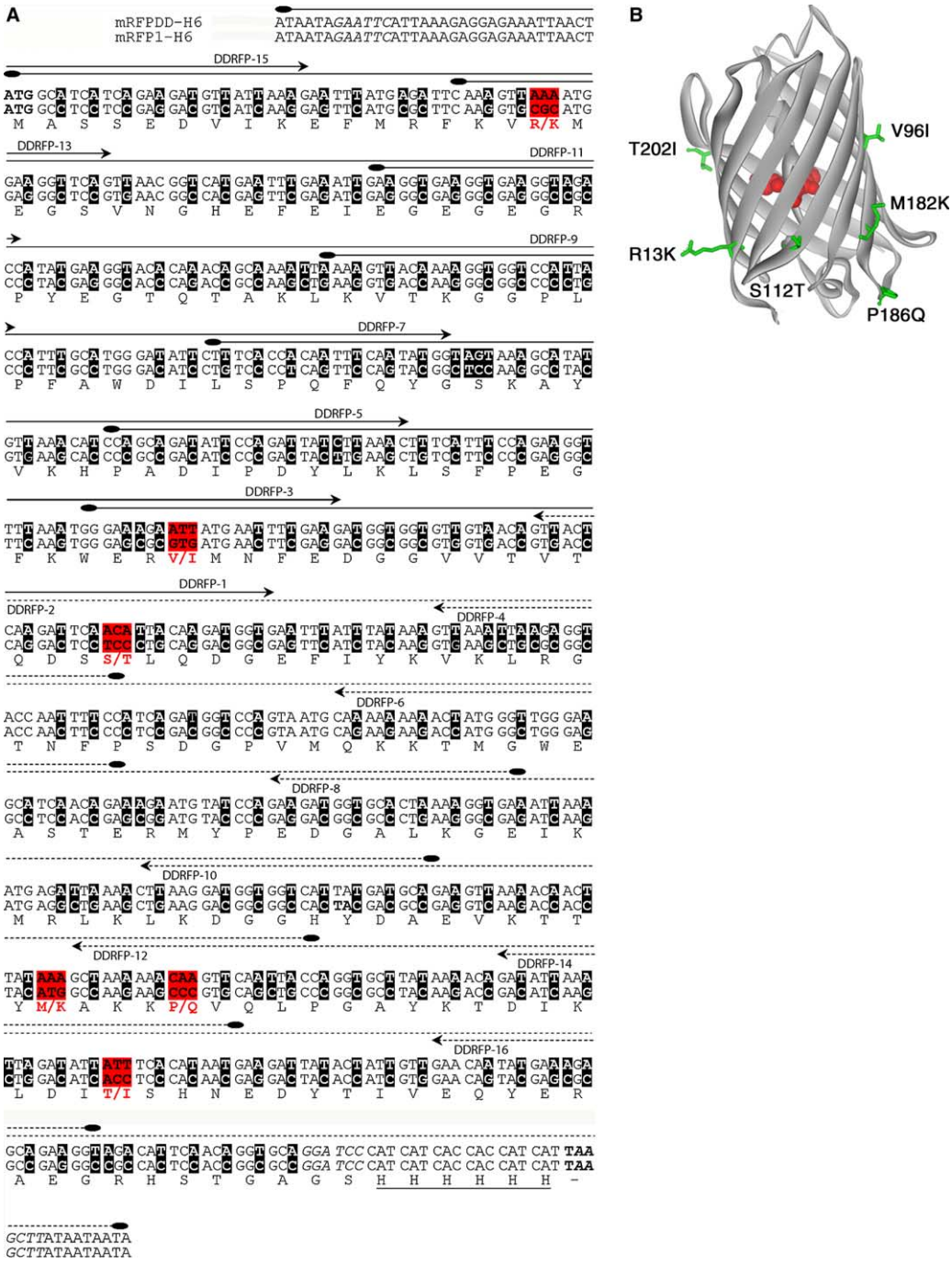

Fig. 1. Construction of mRFPmars based on the sequence of mRFP1. (A) Alignment of the mRFP1 DNA sequence (mRFP1-His6) and the synthetic DNA sequence (mRFPmars-His6) with 5′ and 3′ overhangs, including the synthetic *Eco*RI, *Bam*HI and *Hin*dIII sites (italics). Changed bases are shaded. The protein sequence of mRFPmars is drawn below the aligned DNA sequences. Both sequences contain an additional DNA fragment coding for a hexahistidine tag at their C-termini. The six amino acids changed in accord with the sequence of RedStar are highlighted in red. Oligonucleotides used as forward primers are drawn in continuous lines and reverse primers in dotted lines. The start and stop codons of both sequences are shown in bold letters. (B) Positions of the converted amino-acid residues superimposed on the X-ray structure of one monomer of DsRed adopted from Yarbrough et al. [23]. The DsRed chromophore is drawn in red, the six mutated residues in green. All six residues are located on the surface of the protein.

111-bp fragment was used as the first template, and oligonucleotides were employed in pairs for the elongation of each prior amplificate starting with DDRFP-3 and DDRFP-4 (Fig. 1A) and ending with DDRFP-17 (5′ata ata ata acc atg ggt aag ctt aaa atg gca tca tca gaa gat gtt att aaa gaa ttt atg aga ttc aaa gtt aaa atg g 3′) and DDRFP-18 (5′tat tat tat aga tct gaa ttc gga tcc tgc acc tgt tga atg tct acc ttc tgc tct ttc ata ttg ttc 3′). The complete 729-bps-amplificate was digested with *Nco*I and *Bgl*II (New England Biolabs), cloned into the expression plasmid pNCO113 [10], and used for transformation of *E. coli* XL1-blue cells yielding the strain XL1-pNCO-mRFPmars.

2.2. Construction and expression of mRFPmars-His6 and mRFP1-His6 in E. coli

The plasmid pNCO-mRFPmars was used as a template, and the oligonucleotides DDRFP-15 and DDRFP-16 were used as primers for PCR amplification. The amplified DNA-fragment was digested with

*Eco*RI and *Hin*dIII and cloned into the vector pNCO113, resulting in the plasmid pNCO-mRFPmars-His6 (Fig. 1A).

To express mRFP1 as a reference in *E. coli*, the plasmid pRSETB containing the sequence of mRFP1 provided by Roger Tsien (UCSD, La Jolla, CA, USA) [8] was used as a template for PCR amplification with the primers mRFP1-Rbs-*Eco*RI (5′-ata ata gaa ttc att aaa gag gag aaa tta act atg gcc tcc tcc gag gac gtc atc aag-3′) and mRFP1-His6-*Hin*dIII (5′-tat tat tat aag ctt aat gat ggt ggt gat gat ggg atc cgg cgc cgg tgg agt ggc ggc cct cg-3′). The DNA fragment was cloned as described above, yielding the plasmid pNCO-mRFP1-His6 (Fig. 1A).

The fluorescent proteins mRFP1-His6 and mRFPmars-His6 were expressed in *E. coli* M15 [pRep4] cultivated under shaking at 37 °C up to an optical density of 0.6 at 600 nm (exponential phase). Isopropyl-ß-D-thiogalactoside (IPTG) was added to a final concentration of 2 mM and incubation was continued overnight. The bacteria were harvested by centrifugation, washed with 0.9% NaCl and stored at −20 °C.

2.3. Protein purification

The bacterial pellet was suspended in 50 mM K-phosphate, pH 8.0, and 0.02% sodium azide (buffer A). The suspension was cooled on ice, ultrasonicated and centrifuged at $26\,000 \times g$ for 20 min. The supernatant was applied to a column of Ni^{2+}-chelating Sepharose FF (2.6 × 5 cm, Amersham Pharmacia Biotech, Freiburg, Germany) equilibrated with buffer A. The column was developed with a linear gradient of 0–500 mM imidazole in buffer A. Fractions were analyzed by SDS–gel electrophoresis. Fractions containing fluorescent proteins were combined, concentrated by ultrafiltration and placed onto a Superdex 75 column (2.6 × 60 cm, Amersham Pharmacia Biotech). Elution was performed with 100 mM K-phosphate, pH 7.0, plus 0.02% sodium azide.

2.4. Determination of relative molecular masses of mRFP1-His6 and mRFPmars-His6

Gelfiltration – The native molecular mass was estimated using a Pharmacia FPLC system equipped with a Superdex 75 column (2.6 × 60 cm, Amersham Pharmacia Biotech, Freiburg, Germany). The elution buffer contained 100 mM K-phosphate, pH 7.0. The column was calibrated using the following standard proteins: cytochrome *C* (12.4 kDa), chymotrypsinogen A (25.7 kDa), GFP (26.5 kDa), carbonic anhydrase (30 kDa), ovalbumin (45 kDa), bovine serum albumin (67 kDa), and DsRed (120 kDa).

Non-denaturing polyacrylamide gel electrophoresis – The gels contained 200 mM Na/K-phosphate, pH 7.2, 4% acrylamide, 0.11% bisacrylamide and 0.1% tetramethylethylenediamine.

2.5. Absorption and fluorescence spectra

Absorption spectra were taken using a UV–VIS spectrophotometer (Ultrospec 2000, Amersham Pharmacia Biotech, Freiburg, Germany) and fluorescence spectra with a FluoroMax-2 spectrofluorimeter (Jobin Yvon Horiba, Munich, Germany) at room temperature in 10-mm quartz cuvettes. For quantum yield determination, the fluorescence of protein solutions in 100 mM K-phosphate, pH 7.0, was compared with solutions of sulforhodamine 101 (fluorescence quantum yield: 0.9) [11] and rhodamine 6G (fluorescence quantum yield: 0.95) [12]. Quantum yield calculations were corrected for the refractive index difference between ethanol (η: 1.3605) and water (η: 1.3329).

2.6. Vector constructs for expression in Dictyostelium

Full-length sequences of α-tubulin or partial sequences of either LimE (LimEΔcoil) or the actin-binding domain (ABD120) of *Dictyostelium* filamin, both previously used to localize actin filaments [13,14], were fused in frame to the C-terminus of either the sequence encoding mRFPmars or mRFP1 [8]. The constructs were cloned and expressed under control of an actin-15 promoter using the expression vector pDEXRH [15] and confirmed by sequence analysis.

2.7. Culture conditions and transformation of Dictyostelium cells

Cells of the *Dictyostelium discoideum* strain AX2-214 were cultivated at 23 °C in nutrient medium, either in shaking culture or on Petri dishes. AX2-214 cells were transformed by electroporation with plasmids encoding mRFPmars-LimEΔcoil, using a Bio-Rad gene pulser at 0.8–0.9 kV and 3 μF with 4-mm cuvettes. After 24 h, 10 μg of blasticidin-S (ICN Biomedicals Inc., Costa Mesa, CA, USA) per ml was added for selection. Transformants were cloned on lawns of *E. coli B/2* and those showing expression of mRFPmars-LimEΔcoil were selected. Accordingly, AX2-214 cells were transformed with the plasmid encoding mRFPmars-ABD120, HG1738 cells expressing calnexin-GFP [16] with a vector for expression of mRFPmars-LimEΔcoil, and HG1731 cells expressing histone 2B-GFP with a plasmid for expression of mRFPmars-α-tubulin.

2.8. Confocal microscopy of live cells

For studying the localization of GFP and mRFP fusion proteins, cells were washed twice in 17 mM K–Na-phosphate buffer, pH 6.0, and were transferred to a glass coverslip in an open chamber to record fluorescence in parallel with phase-contrast images. Live cells were observed with a confocal microscope LSM 410 (Zeiss, Jena, Germany) equipped with 488-nm argon and 543-nm neon lasers and a 100×/1.3 Plan-Neofluar objective. In vivo fluorescence spectra were taken on a Zeiss LSM 510 Meta confocal microscope. For dual-wavelength recordings, BP510-525 and HQ607-682 filters were used for the emissions.

To record macropinocytosis, cells were incubated with 0.2 mg per ml of Alexa dextran 488 (MW 10 000; Molecular Probes, Eugene, OR, USA).

2.9. Miscellaneous

DNA was sequenced by the custom sequencing service of GATC Biotech (Konstanz, Germany) or Medigenomix (Martinsried, Germany). N-terminal protein sequencing was performed by the automated Edman method using a 471A Protein Sequencer (Perkin–Elmer). Protein concentration was determined according to [17]. SDS–polyacrylamide gel electrophoresis was performed in 16% gels calibrated with molecular mass standards from Sigma (Munich, Germany). Confocal scans were processed by ImageJ software. Fig. 1B was produced using ViewerLite 5.0 (http://www.accelrys.com).

3. Results

3.1. Synthesis of an improved version of monomeric RFP, mRFPmars

The gene encoding mRFPmars was synthesized by PCR elongation using eight oligonucleotide pairs as primers (Fig. 1A). The synthetic DNA was cloned into the plasmid pNCO113 and verified by sequence analysis (GenBank accession number AY679163). The changes introduced into the mRFP1 coding sequence to generate the synthetic mRFPmars gene are outlined in Fig. 1A. Six of the changed codons alter the amino-acid sequence in accord with the changes introduced into RedStar [9]. A seventh amino acid altered in RedStar, F125L, coincided with the exchange introduced into the mRFP1 sequence [8]. All six amino-acid residues adopted from RedStar are located on the surface of the RFP molecule (Fig. 1B).

202 codons (90%) were adapted to the preferred *Dictyostelium* codon usage without altering the amino-acid sequence. In that way, the GC content of the synthetic gene was decreased from 64% to 31%, a value in the range of the average genomic GC level of *Dictyostelium* [18].

To facilitate purification of mRFPmars and mRFP1, we cloned the two genes into a bacterial expression vector, enabling the synthesis of each protein with a hexa-histidine tag fused to their C-terminal ends. After induction in *E. coli*, the abundant synthesis of proteins with a molecular mass of about 26 kDa was detectable. The recombinant fusion proteins were purified on Ni-chelating Sepharose FF columns. Both proteins showed one single band on non-denaturing polyacrylamide gels (Fig. 2), whereas on SDS–PAGE two additional bands at ~7 and ~19 kDa were observed. The fragmentation is in line with the previous observation that the C=N bond in the acylimine group of the chromophore irreversibly hydrolyzes upon boiling before performing the SDS–PAGE [19].

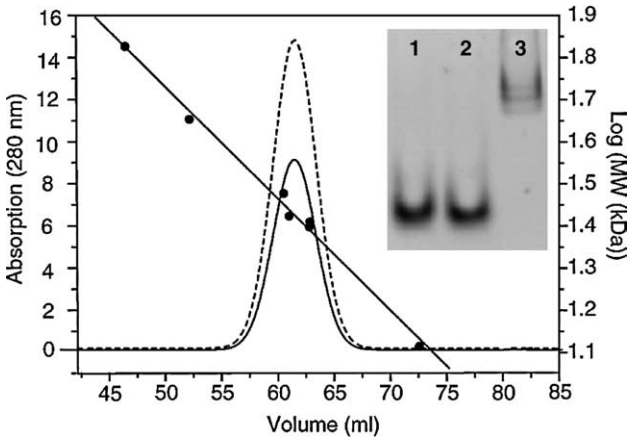

Fig. 2. Scaled elution profile of mRFPmars-His6 (continuous line) and mRFP1-His6 (dashed line). Proteins were placed on top of a Superdex 75 column and were eluted with 100 mM K-phosphate, pH 7.0. The column was calibrated (straight line) using six standard proteins (Section 2.4) plus DsRed, which eluted in the excluded volume. Inset: 4% native polyacrylamide gel. Lane 1: mRFPmars-His6; lane 2: mRFP1-His6; lane 3: DsRed.

The native molecular mass of mRFPmars was estimated using an FPLC system equipped with a Superdex 75 gel filtration column calibrated using standard proteins including mRFP1, which is known to be monomeric, and DsRed, which forms tetramers with a molecular mass of about 100 kDa. mRFP1 and mRFPmars both eluted at 61.5 ml from the column, corresponding to a molecular mass of 26.6 kDa in accord with the calculated molecular mass of 26.4 kDa (Fig. 2). The separation range of the column used comprises 3–70 kDa in a total volume of 30–120 ml. Hence, the tetrameric DsRed eluted within the excluded volume.

When analyzed by non-denaturing gel electrophoresis at pH 7.2, the mobility of mRFPmars was slightly decreased relative to mRFP1 (Fig. 2). This observation can be explained by the replacement of methionine 182 by the positively charged lysine in mRFPmars (calculated isoelectric points: mRFP1, 6.13; mRFPmars, 6.28). As a consequence of the 4-fold molecular mass of DsRed, this reference protein was clearly separated from mRFP1 and mRFPmars using native PAGE.

The absorption spectra of mRFP1 and mRFPmars showed no remarkable difference (Fig. 3A), and were almost identical to the previously published absorption spectrum of mRFP1 [8]. At pH 7.0, both proteins showed absorption maxima at 585 nm, a lower peak at 503 nm, and a shoulder around 550 nm. Extinction coefficients (ε) at 585 nm were 32 557 $M^{-1}\,cm^{-1}$ for mRFPmars and 33 943 $M^{-1}\,cm^{-1}$ for mRFP1 at pH 7.0. Identical fluorescence quantum yields were determined for the two proteins (data not shown).

The absorption and emission spectra of mRFPmars are composed of peaks in the longer wavelength range (>525 nm) that are weakly affected by pH-changes, and peaks in the shorter wavelength range that are strongly pH-dependent (Fig. 3B). Weakly pH-dependent is the major absorption peak of mRFPmars at 585 nm and the highest emission peak at 602 nm. The absorption peak at 503 nm corresponds to the emission peak at 515 nm. A rise of pH leads to an increase of both peaks. The suppression of these peaks at low pH indicates that they belong to the deprotonated form of the protein. The protonated

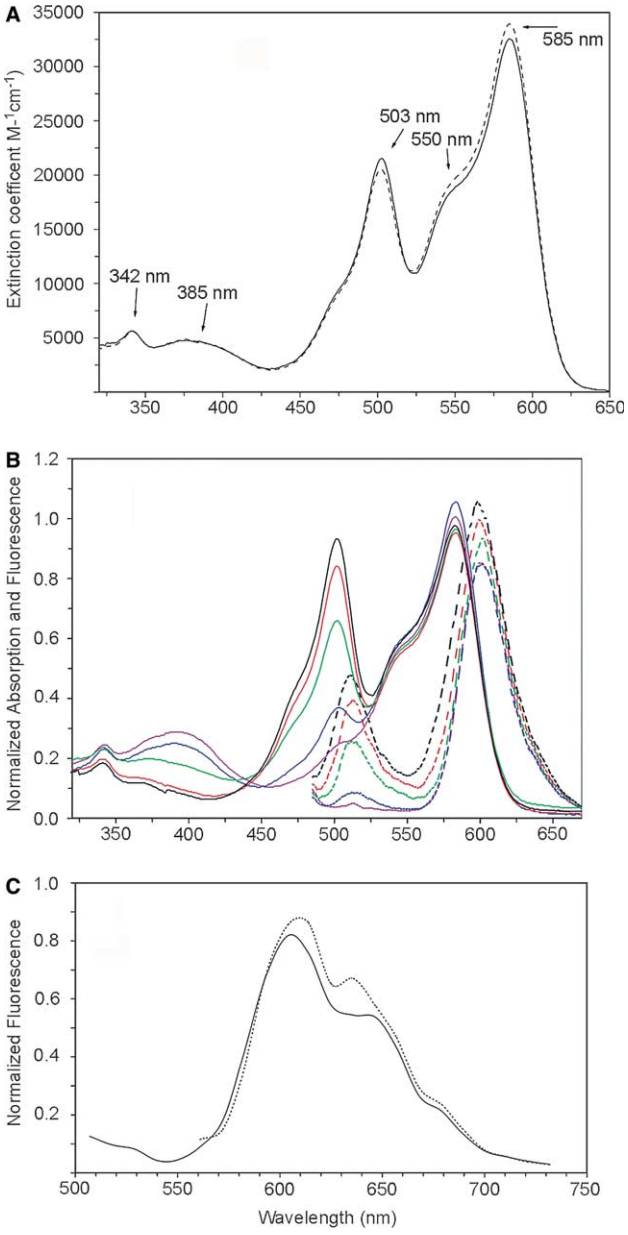

Fig. 3. Absorption and emission spectra of mRFPmars. (A) Comparison of the absorption spectra of mRFPmars and mRFP1. Solutions in 100 mM K-phosphate, pH 7.0, contained equal concentrations of the two proteins. (B) Absorption spectra (continuous lines) and emission spectra (dashed lines) of mRFPmars-His6 at different pH-values. 250 μl of protein solutions was dialyzed against 50 ml of 100 mM K-phosphate buffers with different pH-values (5.0: magenta; 6.0: blue; 7.0: green; 8.0: red; and 9.0: black). The excitation wavelength was 480 nm. (C) Emission spectra of live *Dictyostelium* cells expressing mRFPmars-LimEΔcoil fusion protein taken with excitation at 488 nm (solid line) or 543 nm (dotted line).

form of this protein is obviously responsible for the absorption peak at 385 nm, which shows inverse pH-dependence and is linked to the 503-nm peak through an isosbestic point at 440 nm.

3.2. *mRFPmars as a red fluorescent tag for double labeling of Dictyostelium cells*

To assess the versatility of mRFPmars for double labeling of eukaryotic cells, we expressed in *Dictyostelium* three mRFP-

mars fusion proteins that paralleled GFP-fusions of the same proteins used in previous studies. LimEΔcoil is a high-affinity probe for filamentous actin network structures [14], ABD120 is the actin-filament binding domain of *Dictyostelium* filamin [13], and α-tubulin is incorporated into microtubules over their entire length [20]. Emission spectra taken with excitation of 488 nm and 543 nm in live cells expressing mRFPmars-LimEΔcoil showed a maximum around 610 nm (Fig. 3C), similar to the spectra obtained for mRFPmars purified from *E. coli*. In *Dictyostelium*, mRFPmars showed minimal green fluorescence of an emission maximum around 520 nm. The localization of the mRFPmars-LimEΔcoil fusion protein corresponded to that of GFP-LimEΔcoil, which has been shown to visualize filamentous actin structures [14].

For double labeling, we expressed mRFPmars-LimEΔcoil together with calnexin-GFP [16] and recorded the fluorescences of both fusion proteins simultaneously in living cells (Fig. 4A). The calnexin-GFP label visualizes the ER membranes and is clearly distinguishable from the F-actin containing structures in the cell cortex.

We also tested mRFPmars as a tag for other probes labeling cytoskeletal proteins. mRFPmars-ABD120 is a fusion to the actin-binding domain of *Dictyostelium* filamin, which localizes to filamentous actin. Fig. 4B shows that cells expressing this red fluorescent probe can be used in combination with green fluorescent Alexa 488-dextran, to follow with this fluid-phase marker the involvement of actin in macropinocytosis [21]. A large macropinocytic cup decorated with mRFPmars-ABD120 is shown in Fig. 4C.

Furthermore, mRFPmars-α-tubulin was co-expressed with histone-2B-GFP in *Dictyostelium* cells. Labeling of microtubules with mRFPmars and visualizing nuclear DNA by histone-2B-GFP in an interphase cell are shown in Fig. 4D. A telophase stage of mitosis with an elongated spindle and separated chromosomes is presented in Fig. 4E. Fig. 4F shows that consecutive stages of mitosis from prophase to the completion of cytokinesis can be captured in the same cell.

4. Discussion

In order to design an optimized monomeric red fluorescent protein suitable for double-fluorescence imaging in *Dictyostelium*, we have created a synthetic protein, mRFPmars, based upon mutations introduced into the tetrameric DsRed sequence. We show that mRFPmars is monomeric in solution and in live-cell imaging confers bright fluorescence when expressed as a tag on proteins of *Dictyostelium*. Two of the tagged proteins recognize filamentous actin structures and one labels the microtubule system. These mRFPmars-tagged proteins can be visualized in combination with various green fluorescent labels to study the involvement of cytoskeletal proteins in organelle dynamics, endocytosis, and mitosis (Fig. 4).

One set of mutations has been adopted from RedStar, a tetrameric variant of DsRed, which was identified by repeated cycles of random mutagenesis and selection of brightly fluorescing cells of bacteria and yeast [9]. It remained unclear whether the brilliance of the RedStar fluorescence is an intrinsic property of the protein, or is due to an improved compatibility with the heterogeneous environment of the cells

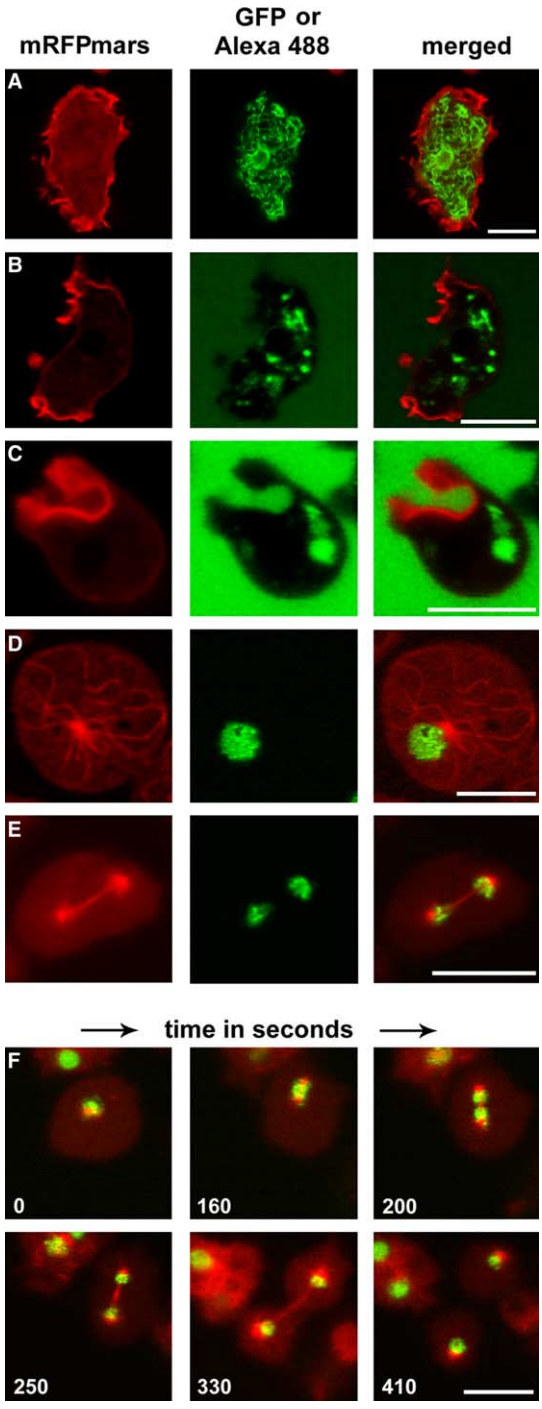

Fig. 4. Dual-wavelength confocal microscopy of *Dictyostelium* cells expressing mRFPmars fusion proteins in combination with green fluorescent labels. (A) Cells expressing LimEΔcoil N-terminally tagged with mRFPmars to visualize the actin cytoskeleton (red) and calnexin-GFP to label the endoplasmic reticulum (green). (B, C) Cells expressing mRFPmars-ABD120 to visualize filamentous actin structures were incubated with Alexa 488 dextran. In B, endosomes are clearly distinguished from cytoskeletal structures. In C, the formation of a macropinocytic cup is shown. (D–F) Cells expressing mRFPmars-α-tubulin and histone-2B-GFP. In D, an interphase cell is depicted with microtubules labeled in red and the nucleus visualized in green. In E, a late stage of mitosis with separated chromosomes and an elongated spindle is shown. In F, consecutive stages of mitosis are captured. Numbers indicate seconds after the recording started: 0, prophase; 160, metaphase; 200–330, ana-/telophase; and 410, almost completed cytokinesis. Bars, 10 μm.

to which this anthozoan protein was transferred. Our measurements of extinction coefficients and of fluorescence quantum yields did not reveal a difference between purified mRFP1 and mRFPmars, suggesting that the mutations introduced from RedStar into the mRFP1 sequence affect the behavior of the protein in vivo rather than the spectral properties of the isolated protein. In line with this notion is the fact that all amino-acid residues converted to generate RedStar are located on the surface of the molecule, this means on the interface between the protein and its cellular environment where folding, maturation, and degradation are controlled (Fig. 1B).

Mature RFP originates from a green-emitting precursor through an additional oxidation step in the chromophore [22,23]. The resulting double bond extends the chromophoric π-system. The fact that the RFP precursor resembles GFP has prompted Matz et al. [24] to suggest that GFP is a regressed version of an ancestral red fluorescent protein that stops maturation at an intermediate green-emitting state. Like GFP, the RFP precursor shows a strong pH-dependence in its absorption spectrum [22]. In GFP, the pH-dependence has been suppressed by the conversion of a tyrosine residue (Y66) in the chromophore to a non-protonable tryptophane residue [22]. This finding suggests that the spectral transitions caused by changing pH are due to the protonation of Y66, a residue that is also present in the mRFP sequence. Based on these data, we assume that the pH-dependent components in the mRFPmars spectra (Fig. 3B) indicate the presence of a GFP-like precursor in the bacterially expressed and purified protein.

In the emission spectrum of *Dictyostelium* cells expressing the fusion protein mRFPmars-LimEΔcoil, the green emission in the 520-nm range proved to be negligible relative to the strong emission at 610 nm (Fig. 3C). This finding is important for the double labeling of cells with proteins that are tagged with mRFPmars or GFP. The low contribution of a green fluorescent component in *Dictyostelium* cells may have two reasons. First, at a cytoplasmic pH around 7.0 the emission is not prominent (green curve in Fig. 3B). Second, within *Dictyostelium* cells the maturation to the red fluorescent state may proceed faster than in bacteria. *Dictyostelium* cells grew at 23 °C whereas the bacteria were cultivated at 37 °C, and lower temperatures tend to improve the maturation [8].

Currently, mRFPmars is the red fluorescent protein of choice for double-labeling experiments using blue, green or yellow fluorescent markers in *Dictyostelium*. We are investigating whether a similar approach for optimization is also applicable to mammalian cells.

Acknowledgements: We thank Jan Faix (LMU München) for providing purified GFP and DsRed protein, Ralph Gräf (LMU München) for help with the LSM 510 Meta microscope, and Klaus Kemnitz (Berlin-Adlershof) for discussion on the fluorescence spectra. The technical assistance of Emmanuel Burghardt and Marlis Fürbringer is gratefully acknowledged. This work was supported by grants from the Deutsche Forschungsgemeinschaft to G.G. and M.F., and from the Fonds der Chemischen Industrie to M.F.

References

[1] Tsien, R.Y. (1998) Ann. Rev. Biochem. 67, 509–544.
[2] Miyawaki, A., Sawano, A., and Kogure, T. (2003) Nat. Cell Biol. Supplement S1-7.
[3] Gerisch, G. and Müller-Taubenberger, A. (2003) Meth. Enzymol. 361, 320–337.
[4] Miyawaki, A. (2003) Dev. Cell 4, 295–305.
[5] Bacia, K. and Schwille, P. (2003) Methods 29, 74–85.
[6] Mizuno, H., Sawano, A., Eli, P., Hama, H. and Miyawaki, A. (2001) Biochemistry 40, 2502–2510.
[7] Baird, G.S., Zacharias, D.A. and Tsien, R.Y. (2000) Proc. Natl. Acad. Sci. USA 97, 11984–11989.
[8] Campbell, R.E., Tour, O., Palmer, A.E., Steinbach, P.A., Baird, G.S., Zacharias, D.A. and Tsien, R.Y. (2002) Proc. Natl. Acad. Sci. USA 99, 7877–7882.
[9] Knop, M., Barr, F., Riedel, C.G., Heckel, T. and Reichel, C. (2002) Biotechniques 33, 592–602.
[10] Stueber, D., Matile, H., and Garotta, G. (1990) Immunological Methods IV (Lefkovits, I., Pernis, P., Eds.), pp. 121–125.
[11] Available from: <http://omlc.ogi.edu/spectra/PhotochemCAD/html/sulforhodamine101.html>.
[12] Kubain, R.F. and Fletscher, A.N. (1982) J. Luminescence 27, 455–462.
[13] Pang, K.M., Lee, E. and Knecht, D.A. (1998) Curr. Biol. 8, 405–408.
[14] Bretschneider, T., Diez, S., Anderson, K., Heuser, J., Clarke, M., Müller-Taubenberger, A., Köhler, J. and Gerisch, G. (2004) Curr. Biol. 14, 1–10.
[15] Faix, J., Gerisch, G. and Noegel, A. (1992) J. Cell Sci. 102, 203–214.
[16] Müller-Taubenberger, A., Lupas, A.N., Li, H., Ecke, M., Simmeth, E. and Gerisch, G. (2001) EMBO J. 20, 6772–6782.
[17] Read, S.M. and Northcote, D.H. (1981) Anal. Biochem. 116, 53–64.
[18] Glöckner, G., Eichinger, L., Szafranski, K., Pachebat, J.A., Bankier, A.T., Dear, P.H., Lehmann, D., Baumgart, C., Parra, G., Abril, J.F., Guigo, R., Kumpf, K., Tunggal, B., Cox, E., Quail, M.A., Platzer, M., Rosenthal, A. and Noegel, A.A. (2002) Nature 418, 79–85.
[19] Gross, L.A., Baird, G.S., Hoffman, R.C., Baldridge, K.K. and Tsien, R.Y. (2000) Proc. Natl. Acad. Sci. USA 97, 11990–11995.
[20] Neujahr, R., Albrecht, R., Köhler, J., Matzner, M., Schwartz, J.M., Westphal, M. and Gerisch, G. (1998) J. Cell Sci. 111, 1227–1240.
[21] Hacker, U., Albrecht, A. and Maniak, M. (1997) J. Cell Sci. 110, 105–112.
[22] Haupts, U., Maiti, S., Schwille, P. and Webb, W.W. (1998) Proc. Natl. Acad. Sci. USA 95, 13573–13578.
[23] Yarbrough, D., Wachter, R.M., Kallio, K., Matz, M.V. and Remington, S.J. (2001) Proc. Natl. Acad. Sci. USA 98, 462–467.
[24] Matz, M.V., Fradkov, A.F., Labas, Y.A., Savitsky, A.P., Zaraisky, A.G., Markelov, M.L. and Lukyanov, S.A. (1999) Nat. Biotechnol. 17, 969–973.